Dynamization at the near cortex in locking plate osteosynthesis by means of dynamic locking screws: an experimental study of transverse tibial osteotomies in sheep

Richter, Henning ; Plecko, Michael ; Andermatt, Daniel ; Frigg, Robert ; Kronen, Peter W ; Klein, Karina ; Nuss, Katja M ; Ferguson, Stephen J ; Stöckle, Ulrich ; von Rechenberg, Brigitte

Abstract: BACKGROUND: Locking plates are widely used in fracture fixation, mainly for meta-diaphyseal fractures, comminuted fractures, fractures with a critical-size bone defect, periprosthetic fractures, osteotomies, and fractures in osteoporotic bone. The aim of this animal study was to evaluate the effect on bone-healing of dynamization of locking plate constructs by means of new 5.0-mm dynamic locking screws (in the DLS group), which allow near-cortex micromotion, compared with a more rigid construct utilizing standard bicortical locking-head screws (in the LS group). Use of dynamic locking screws allows modulation of the stiffness of existing locking compression plate systems via parallel interfragmentary micromotion. METHODS: A standardized diaphyseal tibial osteotomy (90°, 3-mm fracture gap) was performed and stabilized with a six-hole large-fragment locking compression plate in twelve female sheep (six in each group). Radiographs were made postoperatively and then weekly from week three until sacrifice at nine weeks. Macroscopic, biomechanical, histologic, and radiographic assessments and microcomputed tomography were performed. RESULTS: The callus in the tested specimens in the DLS group had better biomechanical stability, with a significantly greater maximum failure moment (mean and standard deviation [SD] as a percentage of intact, 55.15 ± 20.65 compared with 26.80 ± 14.96 in the LS group; p = 0.021). The DLS group also had greater periosteal callus volume at the near cortex (mean volume and SD as a percentage of the tibial shaft volume, 36.21% ± 10.08% compared with 18.98% ± 8.61% in the LS group; p = 0.026) and in the intercortical region (mean volume and SD as a percentage of the bone volume of the tibial shaft, 3.56% ± 0.52% compared with 2.64% ± 0.98% in the LS group; p = 0.045), as shown by microcomputed tomography. The DLS group also had significantly greater torsional stiffness (mean and SD as a percentage of intact, 84.88 ± 13.51 compared with 58.89 ± 20.61 in the LS group; p = 0.027). CONCLUSIONS: Controlled micromotion and nearly homogeneous interfragmentary strain at the fracture site, together with the stable bicortical fixation achieved by the new dynamic locking screw, led to more uniform callus formation, significantly more callus formation at the near cortex, and biomechanically more competent bone-healing compared with use of rigid locking plate constructs with locking-head screws.

DOI: https://doi.org/10.2106/JBJS.M.00529

locking plate osteosynthesis by means of dynamic locking screws: an experimental study of transverse tibial osteotomies in sheep. Journal Bone Joint Surgery America, 97(3):208-215.
DOI: https://doi.org/10.2106/JBJS.M.00529

Dynamization at the Near Cortex in Locking Plate Osteosynthesis by Means of Dynamic Locking Screws

An Experimental Study of Transverse Tibial Osteotomies in Sheep

Henning Richter, DVM*, Michael Plecko, MD*, Daniel Andermatt, Dipl Ing, Robert Frigg, MD, Peter W. Kronen, DVM, Karina Klein, DVM, Katja Nuss, DVM, Stephen J. Ferguson, PhD, Ulrich Stöckle, MD, and Brigitte von Rechenberg, DVM

Investigation performed at the Musculoskeletal Research Unit (MSRU), Equine Hospital, Vetsuisse Faculty, University of Zürich, Zürich, Switzerland

Background: Locking plates are widely used in fracture fixation, mainly for meta-diaphyseal fractures, comminuted fractures, fractures with a critical-size bone defect, periprosthetic fractures, osteotomies, and fractures in osteoporotic bone. The aim of this animal study was to evaluate the effect on bone-healing of dynamization of locking plate constructs by means of new 5.0-mm dynamic locking screws (in the DLS group), which allow near-cortex micromotion, compared with a more rigid construct utilizing standard bicortical locking-head screws (in the LS group). Use of dynamic locking screws allows modulation of the stiffness of existing locking compression plate systems via parallel interfragmentary micromotion.

Methods: A standardized diaphyseal tibial osteotomy (90°, 3-mm fracture gap) was performed and stabilized with a six-hole large-fragment locking compression plate in twelve female sheep (six in each group). Radiographs were made postoperatively and then weekly from week three until sacrifice at nine weeks. Macroscopic, biomechanical, histologic, and radiographic assessments and microcomputed tomography were performed.

Results: The callus in the tested specimens in the DLS group had better biomechanical stability, with a significantly greater maximum failure moment (mean and standard deviation [SD] as a percentage of intact, 55.15 ± 20.65 compared with 26.80 ± 14.96 in the LS group; p = 0.021). The DLS group also had greater periosteal callus volume at the near cortex (mean volume and SD as a percentage of the tibial shaft volume, 36.21% ± 10.08% compared with 18.98% ± 8.61% in the LS group; p = 0.026) and in the intercortical region (mean volume and SD as a percentage of the bone volume of the tibial shaft, 3.56% ± 0.52% compared with 2.64% ± 0.98% in the LS group; p = 0.045), as shown by microcomputed tomography. The DLS group also had significantly greater torsional stiffness (mean and SD as a percentage of intact, 84.88 ± 13.51 compared with 58.89 ± 20.61 in the LS group; p = 0.027).

Conclusions: Controlled micromotion and nearly homogeneous interfragmentary strain at the fracture site, together with the stable bicortical fixation achieved by the new dynamic locking screw, led to more uniform callus formation, significantly more callus formation at the near cortex, and biomechanically more competent bone-healing compared with use of rigid locking plate constructs with locking-head screws.

Peer Review: This article was reviewed by the Editor-in-Chief and one Deputy Editor, and it underwent blinded review by two or more outside experts. It was also reviewed by an expert in methodology and statistics. The Deputy Editor reviewed each revision of the article, and it underwent a final review by the Editor-in-Chief prior to publication. Final corrections and clarifications occurred during one or more exchanges between the author(s) and copyeditors.

The use of locking compression plates and locking-head screws for fracture stabilization has contributed to modern minimally invasive osteosynthesis. Although intramedullary nailing is the predominant method used to stabilize diaphyseal fractures, locking plates are advocated for the treatment of meta-diaphyseal fractures, comminuted fractures, fractures with a critical-size bone defect, periprosthetic fractures, and osteotomies as well as fractures in osteoporotic bone[1-7]. With

*Henning Richter, DVM, and Michael Plecko, MD, contributed equally to the writing of this article.

Disclosure: One or more of the authors received payments or services, either directly or indirectly (i.e., via his or her institution), from a third party in support of an aspect of this work. None of the authors, or their institution(s), have had any financial relationship, in the thirty-six months prior to submission of this work, with any entity in the biomedical arena that could be perceived to influence or have the potential to influence what is written in this work. One or more of the authors has had another relationship, or has engaged in another activity, that could be perceived to influence or have the potential to influence what is written in this work. The complete **Disclosures of Potential Conflicts of Interest** submitted by authors are always provided with the online version of the article.

locking screw fixation, the fracture region itself is not grossly disturbed. This allows biological fracture-healing while the locking mechanism takes over the mechanical load and thus minimizes the micromotion at the fracture site. Nevertheless, substantial complication rates have been reported[8-11]. The rigidity at the fracture site is believed to be responsible for delayed callus formation, especially at the near cortex, leading to reported delayed unions or nonunions[12-16]. Increasing the working length (i.e., the distance from the first screw to the fracture line)[17] and thereby reducing the rigidity of the plate-screw construct will substantially increase micromotion at the far cortex without a comparable stimulus at the near cortex, leading to asymmetric interfragmentary strain (see Appendix). To address this difficulty, a recently developed dynamic locking screw (DLS; DePuy Synthes) has been introduced[18,19]; the special sleeve design of the screw maintains the overall mechanical stability of the fracture while allowing micromotion at the fracture site itself. The DLS is anchored in both cortices. The screw head is fixed within the plate hole, providing angular stability, while the sleeve-pin nature of the construct allows controlled micromotion (see Appendix). Interfragmentary strain is thereby more symmetrically distributed within the fracture gap (Fig. 1).

Similar approaches for increasing near-cortex micromotion have been pursued by means of the far-cortex locking screw developed by Bottlang et al.[20] and the near-cortex slotted holes introduced by Gardner et al.[21,22]. However, both of those techniques focus only on screw purchase in the opposite cortex.

In addition to fracture type, the bone biology, local blood supply, and additional soft-tissue damage[23], interfragmentary micromotion at the fracture site can either accelerate or delay fracture-healing[24,25]. The outcome is dependent on the degree and direction of micromotion between the fragments and/or the size of the fracture gap. Fixation that allows either too little[26] or too much[27-29] micromotion can inhibit callus and new bone formation at the fracture site. Axial motion has a positive effect, and the effect of shear forces has not been definitely established, as some authors have reported a negative effect of shear and torsional motions on bone formation at the fracture gap[23,26,28,30-32], but other authors have demonstrated a positive effect[33,34]. The fracture-healing response represents a very complex situation and can be stimulated by a wide range of interfragmentary motion. Cyclic compression leads to significantly more callus formation compared with cyclic distraction[35]. Interfragmentary motion also creates tissue tension and hydrostatic pressure between the fracture ends, eliciting periosteal and endosteal cell activation. According to the interfragmentary strain theory, the determining factor for tissue differentiation is the strain (deformation) experienced by the repair tissue (where strain = interfragmentary motion/gap size). The optimal strain value for fracture-healing is expected to be between 2% and 10%[36]. The optimal axial movement is thought to be 0.2 to 1.0 mm[28,32]. The DLS achieves the appropriate range of interfragmentary motion by means of a specific design feature, consisting of a core pin and a threaded sleeve, that allows for axial movement and bicortical anchorage with increased micromotion at the near cortex[18,19].

Experimental studies in sheep with oblique tibial osteotomies with 0, 1, and 3-mm gaps stabilized with a 3.5-mm locking compression plate system revealed more homogeneously increased, more symmetrical, and smoother callus formation at the near cortex, as well as improved biomechanical stability, in the group treated with a dynamic locking screw compared with the control group[19,37]. However, conclusions could not be drawn regarding transverse fractures, in which interfragmentary motion takes place in a smaller, more compact region. In addition, the implant stiffness of a small-fragment 3.5-mm veterinary locking compression plate fixed with 3.5 and 3.7-mm screws definitely differs from that of a large-fragment locking compression plate fixed with 5.0-mm locking screws in humans. As established by biomechanical testing, the dynamization effect is more pronounced in the stiffer large-fragment implant. Therefore, the goal of the present study was to assess the influence of a more dynamic fixation approach on callus formation at the fracture gap in sheep that underwent transverse tibial osteotomy and fracture fixation with a 5.0-mm large-fragment titanium locking compression plate and either dynamic locking screws or locking-head screws.

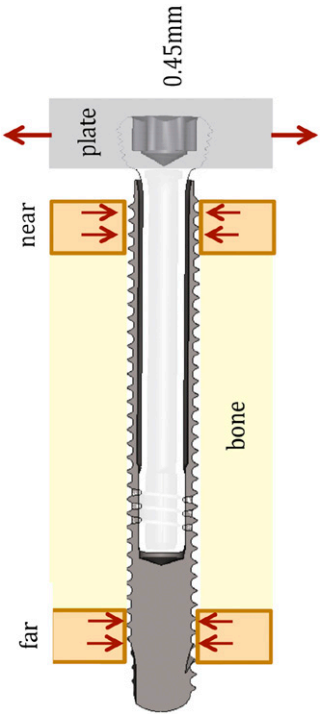

Fig. 1
Schematic showing the bone-screw and screw-plate interfaces of a DLS construct. The maximum micromotion at the near cortex is 0.45 mm.

Material and Methods

Major aspects of the study are outlined below. Further details of the experimental protocol are given in the Appendix.

Animal Experiments

Implants

A six-hole, large-fragment, pure-titanium locking compression plate (LCP; Synthes) was used in combination with either six dynamic locking screws (DLS) in the DLS group or six locking-head screws (LS; Synthes) in the LS group (see Appendix). A custom-made LCP-shaped cutting guide with parallel guiding

slots for the osteotomy blade ensured a standardized 3-mm gap, and a distance holder could be interposed at the fracture site to ensure a symmetrical 3-mm gap. Small rubber rings were used around the plate to achieve a standardized distance of 2 mm from the bone surface to the overlying plate.

Experimental Animals

Thirteen female Swiss-Alpine sheep (twelve, plus one reserve) with a mean age (and standard deviation [SD]) of 2.5 ± 0.5 years and weight of 74.3 ± 4.99 kg were used in the study, which was conducted according to Swiss laws for animal welfare and approved by the local governmental authorities. Animals were randomly assigned to two groups of six animals each; the only difference in the procedure was the use of dynamic locking screws for fixation in the test (DLS) group and locking-head screws in the control (LS) group.

During recovery, the animals were kept in a suspension system for three weeks, as this was known to be a critical phase. Although the sling prevented the animals from lying down and getting up, the limbs of the animals bore their entire weight. The animals were subsequently permitted to roam freely in large six-sheep pens until sacrificed at nine weeks after surgery.

Surgical Procedure

Anesthesia was induced through a jugular catheter and was maintained with an intravenous constant-rate infusion plus isoflurane inhalation. Analgesics were administered perioperatively and were continued for three days postoperatively. Antibiotics and tetanus serum were administered prophylactically.

Following disinfection and sterile draping, a 15 to 18-cm skin incision was made on the medial aspect of the tibia. The subcutaneous tissue and fascia were incised, and the medial shaft of the tibia was exposed.

The plate was slightly contoured to fit the tibial shaft. The cutting guide, with the rubber rings in place, was first temporarily fixed to the bone with Kirschner wires at both ends and was then temporarily fixed to the intact tibia with four unicortical screws (two proximal and two distal). An oscillating saw was used to perform the osteotomy through the guiding slots under constant irrigation with 0.9% NaCl solution. After the template was removed, the fragments were repositioned and fixed with a six-hole LCP, utilizing the 3-mm distance holder to ensure a standardized parallel gap. The six drill holes were made with use of a 4.3-mm drill bit, and 5.0-mm bicortical screws (DLS or LS type, depending on the group) were inserted with use of a torque-limited (4-Nm) screwdriver. After fixation of the plate, the rubber rings were cut, stretched, and removed, with protection of the periosteum. Routine closure of the fascia and subcutaneous tissue was performed, and staples were used for skin closure. A cast extending distally from the stifle joint was applied, and full weight-bearing was started on the day of surgery. Bandages were changed at week three and then weekly at the time of radiography.

Diagnostic Imaging

Radiographs (24 × 30 cm) were made in the mediolateral (270°) and anteroposterior (0°) directions at the end of the operative procedure to confirm correct implantation. Approximately mediolateral radiographs were made weekly from postoperative week three until the time of sacrifice; these were angled by 5° in the anterior and posterior directions (i.e., 265° and 275°) for better visualization of the near cortex.

Harvesting of Samples

The tibiae were harvested immediately after sacrifice of the animals at week nine. After dissection of the surrounding soft tissue, the macroscopic appearance of callus formation was documented, and the implants were then removed.

Biomechanical Testing After Implant Removal

The proximal and distal ends of each tibia were embedded in PMMA (polymethylmethacrylate), leaving the same exposed section (100 to 150 mm in length) for each pair of tibiae, and the samples were subjected to torsional testing. Loading was in internal rotation, with a constant angular velocity of 5°/min until failure. The contralateral, intact tibia served as the control. Torsional stiffness was calculated by a linear fit to the experimental data from 0 to 10 Nm. (Two pairs of specimens had low failure moments of 6.73 and 7.06 Nm; in these cases, the stiffness calculations had to be restricted to ranges of 0 to 6.5 and 0 to 7.0 Nm, respectively.)

Processing of Histologic Samples

After testing, the fracture site was excised by cutting at the levels of the second and fifth screws, and the resulting bone block was fixed in 40% ethanol for histologic analysis. The sample was prepared for nondecalcified histology and embedded in a plastic section as described previously[19]. After dehydration in an ascending series of ethanol baths (40% to 100%), the sample was defatted in xylene and infiltrated with PMMA precursors before the mold was polymerized. A cut was made in the middle of the longitudinal axis of the bone block, at a 90° angle to the plate, with use of a diamond saw. After grinding and mounting on special PMMA slides, 300-μm sections were stained with toluidine blue.

Evaluation

Radiographs

Interpretation of the radiographs was performed by two blinded, independent senior consultant radiologists. Quantitative analysis of all radiographs from weeks three through nine was performed with use of specialized computer imaging software. The callus was outlined at a standardized magnification. Total callus area and mean, minimum, and maximum callus density were recorded. To compensate for possible variations among radiographs, callus density results were normalized by multiplying them by the density index for that radiograph (x). The index was calculated from the mean density within the extremity and the mean value of the background outside the extremity (which served as the control value) according to the following equation: $Index_x = (Density_x - Density_{x,air})/Density_x$.

Microcomputed Tomography (μCT)

Quantitative assessment of the bone samples fixed in 70% ethanol was performed with use of μCT (70 kVp, 200-ms exposure time). All projections were measured twice, and mean values were calculated. The orientation of the sample was controlled by foam support elements so that the longitudinal axis of the tibia was coincident with the μCT rotational axis. A Gaussian three-dimensional filter was used to minimize noise, and a thresholding algorithm was used for segmentation of bone relative to background and for segmentation of callus relative to adjacent normal bone (which was more mineralized and appeared denser). Masking was performed on the basis of the segmentation thresholds to identify volumes of interest (see Appendix), which were analyzed with use of standardized morphometric algorithms. Parameters measured included bone density; total tibial shaft volume; total callus volume; periosteal (outer) callus volume; endosteal, near-cortex, and far-cortex callus volumes; total volume of the near and far cortices; and callus volume bridging the fracture gap (not including the surrounding periosteal callus), expressed both as the total gap callus (including callus bridging the bone marrow) and as the ring gap (intercortical) callus (not including callus bridging the bone marrow).

Histology

The toluidine blue-stained sections were evaluated with use of a light microscope with a mounted digital camera. Photographs were taken at a standardized magnification and digitized. All histomorphometric evaluations were performed manually by the same author (H.R.), who was blinded with regard to the treatment group and had been trained by a senior staff member. Qualitative evaluation included the type and distribution of callus as well as the presence of osteochondral ossification and granulation tissue (mesenchymal and vascular tissue, including bone marrow).

The digitized photographs were further processed in Photoshop (version 4.0; Adobe) by color-coding the various regions. The regions were automatically detected and measured in a standardized fashion by a macro created in customized evaluation software (QWin; Leica Microsystems). The resulting areas were expressed as a percentage of the total measured bone area.

The endosteal, near-cortex, and far-cortex components of the total periosteal and endosteal callus were further distinguished by separate colors. The resulting areas were expressed as a percentage of the total area of periosteal and endosteal callus. (The intercortical callus, or callus bridging the gap in the cortex in this two-dimensional histomorphometric evaluation, represents a slice out of the volume of ring gap callus described above in the μCT section.)

Finally, the various components of old and new bone matrix as well as granulation tissue in the intercortical callus in the osteotomy gap were colored

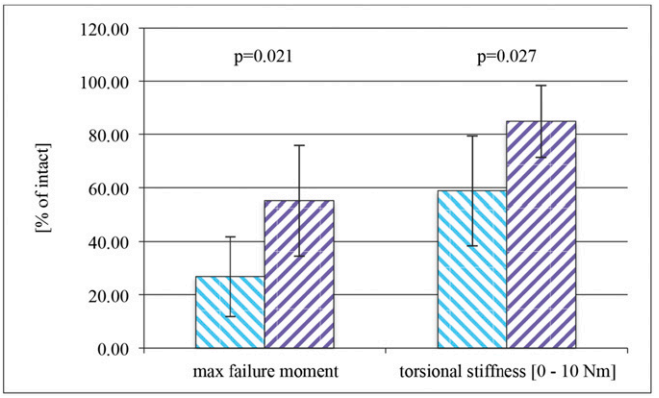

Fig. 2

Torsion test data (mean and SD). Light blue = LS, and violet = DLS.

and measured separately. The resulting areas were expressed as a percentage of the total intercortical callus area.

Microradiography

Microradiographs were evaluated by direct comparison to the toluidine blue-stained histology sections. The evaluation focused on callus size, distribution, and homogeneity as well as the presence of nonunions.

Statistical Analysis

The Student t test was used to assess differences between groups and over time. A p value of ≤0.05 was considered significant.

Source of Funding

This animal study was funded by DePuy Synthes (Solothurn, Switzerland), and two of the authors are employees of that company. This study was also funded by a grant from the Schweizerischer Nationalfond (Swiss National Science Foundation) for doctoral students and a grant from the University of Zurich Veterinary Hospital.

Results

There were no perioperative complications. One animal (in the LS group) was found to have sustained a spiral fracture through the proximal screws at three weeks postoperatively; it was removed from the study and was replaced. Macroscopic evaluation of the tibiae revealed that all osteotomy sites had callus formation and all implants were firmly seated at the time of sacrifice.

Biomechanical Testing After Implant Removal

The range in torsional stiffness was considerable (26.2 to 79.2 Nm/deg in the LS group and 69.4 to 109 Nm/deg in the DLS group). However, mean torsional stiffness, relative to the intact value, was significantly higher in the DLS group than in the LS group (mean and SD as a percentage of intact, 84.88 ± 13.51 compared with 58.89 ± 20.61 in the LS group; p = 0.027). The testing to failure of the callus revealed a significantly greater mean failure load in the DLS group (55.15% ± 20.65%) than in the LS group (150% ± 14.96% of intact, p = 0.021) (Fig. 2).

Test	 total callus mean ± SD * significant DLS/LS (p=0.026)	 outer callus mean ± SD * significant DLS/LS (p=0.026)	 gap callus mean ± SD * significant DLS/LS (p=0.045)
VOI	C.BV/S.TV [%]	O.BV/S.TV [%]	G.BV/S.BV [%]
D L S	36.21* ± 10.08	26.72* ± 9.63	3.56* ± 0.52
L S	18.98 ± 8.61	10.67 ± 7.27	2.64 ± 0.98

Fig. 3

Significantly different μCT morphometric parameters at the near cortex. VOI = volume of interest, C.BV/S.TV = total callus volume normalized relative to the total tibial shaft volume, O.BV/S.TV = periosteal callus volume normalized relative to the total tibial shaft volume, and G.BV/S.BV = intercortical callus volume normalized relative to the bone volume of the tibial shaft.

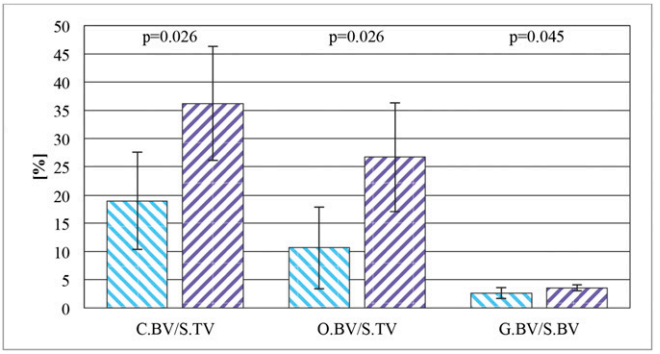

Fig. 4

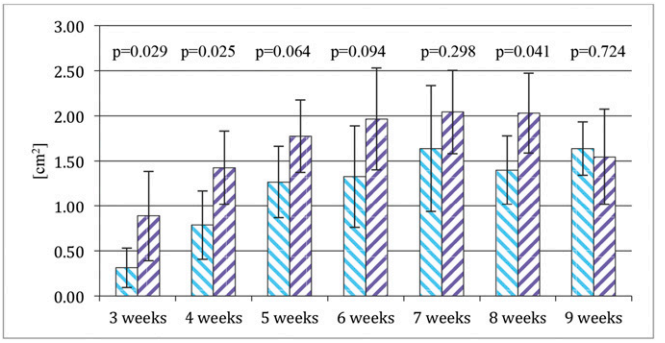

Fig. 5

Fig. 4 Significantly different μCT morphometric parameters at the near cortex (mean and SD). C.BV/S.TV = total callus volume normalized relative to the total tibial shaft volume, O.BV/S.TV = periosteal callus volume normalized relative to the total tibial shaft volume, and G.BV/S.BV = intercortical callus volume normalized relative to the bone volume of the tibial shaft. Light blue = LS, and violet = DLS. **Fig. 5** Callus area (mean and SD) observed in the 275° radiographs at weeks three through nine. Light blue = LS, and violet = DLS.

Diagnostic Imaging

Although the total volume and density of the tibial shaft in the two study groups were similar, three of the other μCT parameters differed significantly between the groups (Figs. 3 and 4). The DLS group showed significantly greater total callus volume and periosteal callus volume at the near cortex (mean volume and SD as a percentage of the tibial shaft volume, 36.21% ± 10.08% compared with 18.98% ± 8.61% in the LS group; $p = 0.026$). Intercortical callus volume was higher in the DLS group, both overall and at each cortex. Only the difference in callus volume between the two groups at the near cortex reached significance (mean volume and SD as a percentage of the bone volume of the tibial shaft, 3.56% ± 0.52% compared with 2.64% ± 0.98% in the LS group; $p = 0.045$). Nevertheless, when the percentage of callus volume at the far cortex was normalized to that of the LS group, the DLS group showed an increase of 140%.

Quantitative evaluation of the radiographs (Fig. 5) demonstrated that the mediolateral radiographs taken at a slight angle (275°) were very valuable. There was a steady increase in callus area in both groups from week three to week seven, which was followed by a decrease until week nine in the DLS group. The LS group exhibited large variations at weeks seven, eight, and nine, without a trend during that time period. At week nine, the callus of both groups again reached a similar level. At weeks three ($p = 0.029$), four ($p = 0.025$), and eight ($p = 0.041$), the amount of callus was significantly greater in the DLS group than in the LS group.

Histology

Overall, the toluidine blue-stained ground sections showed callus formation at both cortices as well as in the intercortical region between the bone fragments in both groups at nine weeks. Tissue within the callus consisted of new bone matrix, mostly new woven bone with few regions still undergoing osteochondral ossification. In both groups, the amount of callus at the near cortex was significantly less than that at the far cortex ($p < 0.001$), mainly because of the overlying plate. Both groups exhibited endosteal callus formation (mean, 31.30% ± 4.92% in the DLS group and 27.04% ± 12.01% in the LS group).

Overall, granulation tissue was the largest tissue component in both groups (Fig. 6).

In both groups, the callus at the far cortex was significantly larger than that at the near cortex ($p < 0.001$) (Figs. 7

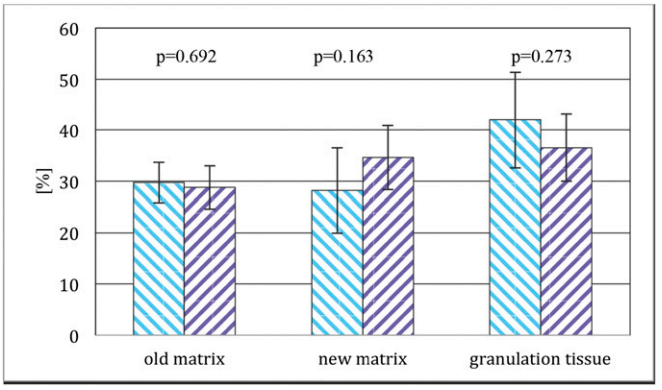

Fig. 6

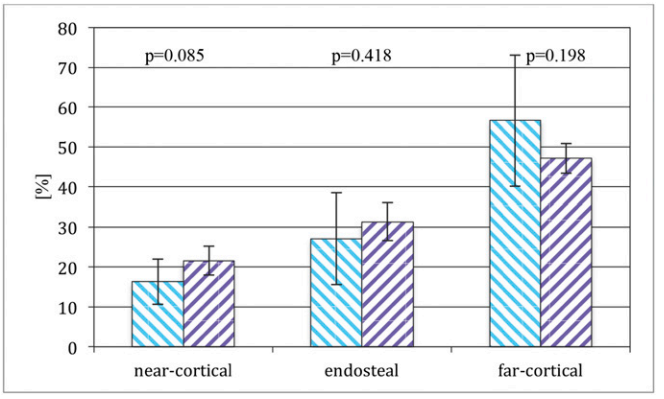

Fig. 7

Fig. 6 Histomorphometric composition in each group (mean and SD). Light blue = LS, and violet = DLS. **Fig. 7** Proportion of callus in each region (mean and SD). Light blue = LS, and violet = DLS.

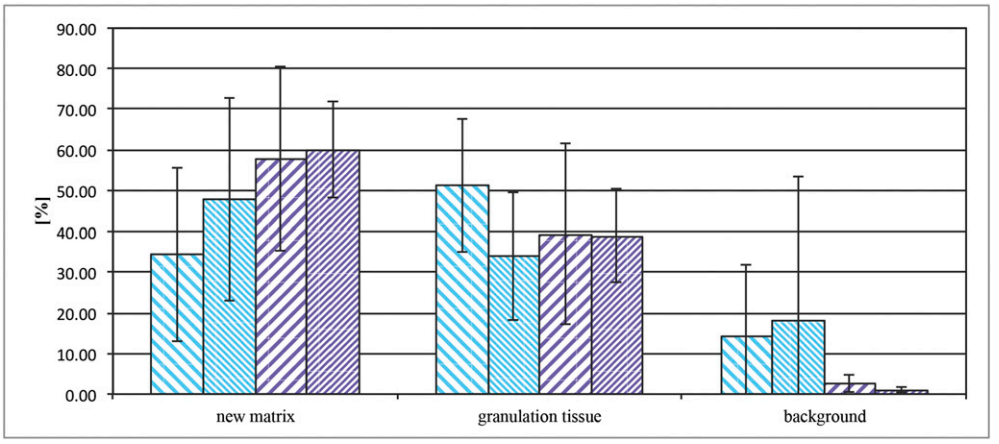

Fig. 8

Histomorphometric composition in each group at the near and far cortices relative to the total area of that cortex (mean and SD). Light blue = LS, and violet = DLS. Wide stripes = near cortex, and narrow stripes = far cortex.

and 8). There was no significant difference in composition between the DLS and LS groups ($p > 0.05$), but the SD for all portions of the callus in the DLS group was remarkably low compared with the LS group.

Microradiography

Calcified callus completely bridged the fracture gap in four of six sheep in the LS group and in five of six sheep in the DLS group. Microfractures resulting from torsion testing to failure in any region of interest were not included in the evaluation.

Discussion

This study investigated the influence of dynamization of a large-fragment locking plate construct, achieved by utilization of new 5.0-mm dynamic locking screws, on bone-healing. A model involving transverse osteotomy in sheep tibiae was used so that our results could be compared with those of several other studies[19,26,27,31,38,39], despite the limited comparability of this model to humans, in whom age, osteoporosis, and various biological factors such as blood supply and soft-tissue damage may influence callus formation.

As in previous biomechanical studies[18], the dynamic locking screw reduced the axial stiffness of the overall construct, leading to a more homogeneous distribution of interfragmentary strain. We hypothesized that this more homogeneous strain would lead to more homogeneous callus formation, and that it would help to overcome the lack of callus formation near the plate as observed in humans[10,15] and replicated in animal studies in which locking plates with locking-head screws have been used[38,39].

The results of this study demonstrated that dynamization of a transverse tibial osteotomy by means of dynamic locking screws rather than locking-head screws leads to increased callus formation at the near cortex and to improvements in stiffness and torsion failure load at nine weeks. In addition to the greater callus at the near cortex, significant increases in total callus volume and callus in the intercortical region demonstrated the improvement in bone-healing. These results are in line with those of Bottlang et al., who reported that far-cortex locking constructs yielded nearly parallel interfragmentary motion of sufficient magnitude to reliably stimulate callus formation around the entire cortex[38].

Both animal groups in the present study exhibited good consistency among the various outcome measures. Callus formation was greater at the far cortex than at the near cortex in both groups. The reduced amount of callus at the near cortex (in both groups) was due to hindrance of callus formation by the physical presence of the plate. Oblique radiographs facilitated optimal visualization of the near-cortex callus. The radiography results were confirmed by μCT. The DLS group also had more consistent callus formation in the region between the cortices, consistent with the biomechanical testing results. This finding also suggests that interfragmentary motion was more parallel in the DLS group than in the LS group.

The DLS group exhibited greater consistency in callus formation among animals compared with the LS group, both radiographically and histologically (see Appendix). In the LS group, the amount of callus was more variable and the quality (e.g., mineralization) of the callus was more irregular. Not only callus volume but also callus symmetry and quality (density and mineralization) were better in the DLS group, both within the osteotomy gap and periosteally, irrespective of the stage of bone remodeling[15]. We suspect that the early plateau phase observed at week six in the DLS group reflects a faster healing response, resulting in earlier biomechanical stability.

Although dynamic locking screws[18,19] and far-cortex locking screws[20,38] both resulted in superior callus formation compared with standard locking-head screws in validated animal models, there is a major difference regarding fixation strength within the bone. Although dynamic locking screws are fixed in both cortices, far-cortex locking screws are only fixed in one. Bottlang et al. have shown that far-cortex locking screw constructs maintain a strength comparable to that of standard locking constructs in normal and osteoporotic specimens[20], but the thickness of the osseous cortex is often substantially reduced in osteoporotic patients[40]. Consequently, the risk of failure in such patients must be assumed to be higher after unicortical fixation, although this is not clinically evident in

their published data. Reduction of implant rigidity and a limited increase of micromotion at the fracture site through use of dynamization screws of either type should improve bone-healing in osteoporotic fracture situations as well. Moreover, both of these "semirigid" constructs should also be beneficial in terms of reduced loading of the implant-bone interface[12,41].

In conclusion, the present study involving transverse tibial osteotomies in sheep confirmed the hypothesis that controlled dynamization at the near cortex can be achieved by means of dynamic locking screws[18], resulting in a more symmetrical and biomechanically stabler callus at the osteotomy site. Although these results cannot be directly extrapolated to human clinical fracture situations, the potential clinical relevance appears obvious, as improved callus formation would substantially enhance patient mobility. Fracture-healing in humans is influenced not only by the mechanical situation at the fracture gap but also by a number of other potential factors such as local impairment of blood supply, damage to soft tissue, stripping of the periosteum, and poor bone biology. Multicenter clinical studies will be needed to clarify the value of dynamic locking screws in improving the mechanical environment at the fracture site.

Appendix

eA A table detailing the products used in the study and figures illustrating interfragmentary strain in the two constructs, geometric details of the two screw types, and examples of μCT volumes of interest as well as additional microradiographic, histomorphometric, and fluorescence images of the animals in the DLS and LS groups are available with the online version of this article as a data supplement at jbjs.org. ■

Henning Richter, DVM
Karina Klein, DVM
Katja Nuss, DVM
Brigitte von Rechenberg, DVM
Musculoskeletal Research Unit (MSRU),
Equine Hospital, Vetsuisse Faculty,
University of Zürich,
Winterthurerstrasse 260,
8057 Zürich, Switzerland.
E-mail address for H. Richter: henning.richter@uzh.ch.
E-mail address for K. Klein: kklein@vetclinics.uzh.ch.
E-mail address for K. Nuss: katja.nuss@vetclinics.uzh.ch.
E-mail address for B. von Rechenberg: bvonrechenberg@vetclinics.uzh.ch

Michael Plecko, MD
Trauma Hospital Graz UKH),
Göstinger Strasse 24,
8021 Graz, Austria.
E-mail address: Michael.Plecko@usz.ch

Daniel Andermatt, Dipl Ing
Robert Frigg, MD
Synthes GmbH, Luzernstrasse 21,
4528 Zuchwil/Solothurn, Switzerland.
E-mail address for D. Andermatt: Andermatt.Daniel@synthes.com.
E-mail address for R. Frigg: robert.frigg@me.com

Peter W. Kronen, DVM
Veterinary Anaesthesia Services International,
Zürcherstrasse 39,
8400 Winterthur, Switzerland.
E-mail address: peter.kronen@vas-int.com

Stephen J. Ferguson, PhD
Institute for Surgical Technology and Biomechanics,
University of Berne,
Stauffacherstrasse 78,
3014 Berne, Switzerland.
E-mail address: sferguson@ethz.ch

Ulrich Stöckle, MD
Berufsgenossenschaftliche Unfallklinik Tübingen,
Schnarrenbergstrasse 95,
72076 Tübingen, Germany.
E-mail address: ustoeckle@bgu-tuebingen.de

References

1. Brosset T, Pasquier G, Migaud H, Gougeon F. Opening wedge high tibial osteotomy performed without filling the defect but with locking plate fixation (TomoFix™) and early weight-bearing: prospective evaluation of bone union, precision and maintenance of correction in 51 cases. Orthop Traumatol Surg Res. 2011 Nov;97(7):705-11. Epub 2011 Oct 15.

2. Floerkemeier S, Staubli AE, Schroeter S, Goldhahn S, Lobenhoffer P. Outcome after high tibial open-wedge osteotomy: a retrospective evaluation of 533 patients. Knee Surg Sports Traumatol Arthrosc. 2013 Jan;21(1):170-80. Epub 2012 Jun 29.

3. Haidukewych GJ, Ricci W. Locked plating in orthopaedic trauma: a clinical update. J Am Acad Orthop Surg. 2008 Jun;16(6):347-55.

4. Horn C, Döbele S, Vester H, Schäffler A, Lucke M, Stöckle U. Combination of interfragmentary screws and locking plates in distal meta-diaphyseal fractures of the tibia: a retrospective, single-centre pilot study. Injury. 2011 Oct;42(10):1031-7. Epub 2011 Jun 12.

5. Lampropoulou-Adamidou K, Karampinas PK, Chronopoulos E, Vlamis J, Korres DS. Currents of plate osteosynthesis in osteoporotic bone. Eur J Orthop Surg Traumatol. 2014 May;24(4):427-33. Epub 2013 Mar 31.

6. Ricci WM, Bolhofner BR, Loftus T, Cox C, Mitchell S, Borrelli J Jr. Indirect reduction and plate fixation, without grafting, for periprosthetic femoral shaft fractures about a stable intramedullary implant. J Bone Joint Surg Am. 2005 Oct;87(10):2240-5.

7. Strauss EJ, Schwarzkopf R, Kummer F, Egol KA. The current status of locked plating: the good, the bad, and the ugly. J Orthop Trauma. 2008 Aug;22(7):479-86.

8. Button G, Wolinsky P, Hak D. Failure of less invasive stabilization system plates in the distal femur: a report of four cases. J Orthop Trauma. 2004 Sep;18(8):565-70.

9. Ebraheim NA, Liu J, Hashmi SZ, Sochacki KR, Moral MZ, Hirschfeld AG. High complication rate in locking plate fixation of lower periprosthetic distal femur fractures in patients with total knee arthroplasties. J Arthroplasty. 2012 May;27(5):809-13. Epub 2011 Oct 2.

10. Henderson CE, Lujan TJ, Kuhl LL, Bottlang M, Fitzpatrick DC, Marsh JL. 2010 Mid-America Orthopaedic Association Physician in Training Award: healing complications are common after locked plating for distal femur fractures. Clin Orthop Relat Res. 2011 Jun;469(6):1757-65. Epub 2011 Mar 22.

11. Vallier HA, Immler W. Comparison of the 95-degree angled blade plate and the locking condylar plate for the treatment of distal femoral fractures. J Orthop Trauma. 2012 Jun;26(6):327-32.

12. Bogunovic L, Cherney SM, Rothermich MA, Gardner MJ. Biomechanical considerations for surgical stabilization of osteoporotic fractures. Orthop Clin North Am. 2013 Apr;44(2):183-200.

13. Henderson CE, Bottlang M, Marsh JL, Fitzpatrick DC, Madey SM. Does locked plating of periprosthetic supracondylar femur fractures promote bone healing by callus formation? Two cases with opposite outcomes. Iowa Orthop J. 2008;28:73-6.

14. Henderson CE, Lujan T, Bottlang M, Fitzpatrick DC, Madey SM, Marsh JL. Stabilization of distal femur fractures with intramedullary nails and locking plates: differences in callus formation. Iowa Orthop J. 2010;30:61-8.

15. Lujan TJ, Henderson CE, Madey SM, Fitzpatrick DC, Marsh JL, Bottlang M. Locked plating of distal femur fractures leads to inconsistent and asymmetric callus formation. J Orthop Trauma. 2010 Mar;24(3):156-62.

16. Vallier HA, Hennessey TA, Sontich JK, Patterson BM. Failure of LCP condylar plate fixation in the distal part of the femur. A report of six cases. J Bone Joint Surg Am. 2006 Apr;88(4):846-53.

17. Stoffel K, Dieter U, Stachowiak G, Gächter A, Kuster MS. Biomechanical testing of the LCP—how can stability in locked internal fixators be controlled? Injury. 2003 Nov;34(Suppl 2):B11-9.

18. Döbele S, Horn C, Eichhorn S, Buchholtz A, Lenich A, Burgkart R, Nüssler AK, Lucke M, Andermatt D, Koch R, Stöckle U. The dynamic locking screw (DLS) can increase interfragmentary motion on the near cortex of locked plating constructs by reducing the axial stiffness. Langenbecks Arch Surg. 2010 Apr;395(4):421-8. Epub 2010 Apr 1.

19. Plecko M, Lagerpusch N, Andermatt D, Frigg R, Koch R, Sidler M, Kronen P, Klein K, Nuss K, Bürki A, Ferguson SJ, Stoeckle U, Auer JA, von Rechenberg B. The dynamisation of locking plate osteosynthesis by means of dynamic locking screws (DLS)-an experimental study in sheep. Injury. 2013 Oct;44(10):1346-57. Epub 2012 Nov 24.

20. Bottlang M, Doornink J, Fitzpatrick DC, Madey SM. Far cortical locking can reduce stiffness of locked plating constructs while retaining construct strength. J Bone Joint Surg Am. 2009 Aug;91(8):1985-94.

21. Gardner MJ, Nork SE, Huber P, Krieg JC. Stiffness modulation of locking plate constructs using near cortical slotted holes: a preliminary study. J Orthop Trauma. 2009 Apr;23(4):281-7.

22. Gardner MJ, Nork SE, Huber P, Krieg JC. Less rigid stable fracture fixation in osteoporotic bone using locked plates with near cortical slots. Injury. 2010 Jun;41 (6):652-6. Epub 2010 Mar 16.

23. Claes L. [Biologie und Biomechanik der Osteosynthese und Frakturheilung. Orthopädie und Unfallchirurgie up2date] [German]. 2006;1:329-341.

24. Goodship AE, Cunningham JL, Kenwright J. Strain rate and timing of stimulation in mechanical modulation of fracture healing. Clin Orthop Relat Res. 1998 Oct; 355(Suppl):S105-15.

25. Kenwright J, Goodship AE. Controlled mechanical stimulation in the treatment of tibial fractures. Clin Orthop Relat Res. 1989 Apr;241:36-47.

26. Epari DR, Kassi JP, Schell H, Duda GN. Timely fracture-healing requires optimization of axial fixation stability. J Bone Joint Surg Am. 2007 Jul;89(7):1575-85.

27. Claes L, Augat P, Suger G, Wilke HJ. Influence of size and stability of the osteotomy gap on the success of fracture healing. J Orthop Res. 1997 Jul;15(4): 577-84.

28. Claes LE, Heigele CA, Neidlinger-Wilke C, Kaspar D, Seidl W, Margevicius KJ, Augat P. Effects of mechanical factors on the fracture healing process. Clin Orthop Relat Res. 1998 Oct;355(Suppl):S132-47.

29. Gómez-Benito MJ, García-Aznar JM, Kuiper JH, Doblaré M. Influence of fracture gap size on the pattern of long bone healing: a computational study. J Theor Biol. 2005 Jul 7;235(1):105-19.

30. Augat P, Burger J, Schorlemmer S, Henke T, Peraus M, Claes L. Shear movement at the fracture site delays healing in a diaphyseal fracture model. J Orthop Res. 2003 Nov;21(6):1011-7.

31. Kenwright J, Richardson JB, Cunningham JL, White SH, Goodship AE, Adams MA, Magnussen PA, Newman JH. Axial movement and tibial fractures. A controlled randomised trial of treatment. J Bone Joint Surg Br. 1991 Jul;73(4):654-9.

32. Klein P, Schell H, Streitparth F, Heller M, Kassi JP, Kandziora F, Bragulla H, Haas NP, Duda GN. The initial phase of fracture healing is specifically sensitive to mechanical conditions. J Orthop Res. 2003 Jul;21(4):662-9.

33. Bishop NE, van Rhijn M, Tami I, Corveleijn R, Schneider E, Ito K. Shear does not necessarily inhibit bone healing. Clin Orthop Relat Res. 2006 Feb;443:307-14.

34. Park SH, O'Connor K, McKellop H, Sarmiento A. The influence of active shear or compressive motion on fracture-healing. J Bone Joint Surg Am. 1998 Jun;80(6):868-78.

35. Hente R, Füchtmeier B, Schlegel U, Ernstberger A, Perren SM. The influence of cyclic compression and distraction on the healing of experimental tibial fractures. J Orthop Res. 2004 Jul;22(4):709-15.

36. Perren SM. Evolution of the internal fixation of long bone fractures. The scientific basis of biological internal fixation: choosing a new balance between stability and biology. J Bone Joint Surg Br. 2002 Nov;84(8):1093-110.

37. Lagerpusch N. [Die Dynamisierung der winkelstabilen Plattenosteosynthese mit Hilfe der "Dynamic Locking Screw" (DLS) - Eine experimentelle Studie an Schafen. [Dissertation]] [German]. Zürich: Universität Zürich; 2011.

38. Bottlang M, Lesser M, Koerber J, Doornink J, von Rechenberg B, Augat P, Fitzpatrick DC, Madey SM, Marsh JL. Far cortical locking can improve healing of fractures stabilized with locking plates. J Bone Joint Surg Am. 2010 Jul 7;92(7): 1652-60.

39. Plecko M, Lagerpusch N, Pegel B, Andermatt D, Frigg R, Koch R, Sidler M, Kronen P, Klein K, Nuss K, Gedet P, Bürki A, Ferguson SJ, Stoeckle U, Auer JA, von Rechenberg B. The influence of different osteosynthesis configurations with locking compression plates (LCP) on stability and fracture healing after an oblique 45° angle osteotomy. Injury. 2012 Jul;43(7):1041-51. Epub 2012 Jan 28.

40. Gautier E, Sommer C. Guidelines for the clinical application of the LCP. Injury. 2003 Nov;34(Suppl 2):B63-76.

41. Lill H, Hepp P, Korner J, Kassi JP, Verheyden AP, Josten C, Duda GN. Proximal humeral fractures: how stiff should an implant be? A comparative mechanical study with new implants in human specimens. Arch Orthop Trauma Surg. 2003 Apr;123(2-3):74-81. Epub 2003 Feb 12.